A hybrid functional first-principles study on the band structure of non-strained $Ge_{1-x}Sn_x$ alloys*

Xiaohuai Wang(王小怀)[1], Chengzhao Chen(陈城钊)[1], Shengqi Feng(冯胜奇)[1], Xinyuan Wei(魏心源)[2], and Yun Li(李云)[1,†]

[1] *Department of Physics and Electronic Engineering, Hanshan Normal University, Chaozhou* 521041, *China*
[2] *State Key Laboratory of Surface Physics, Fudan University, Shanghai* 200433, *China*

(Received 24 July 2017; revised manuscript received 26 August 2017; published online 20 November 2017)

Using hybrid-functional first-principles calculation combined with the supercell method and band unfolding technique we investigate the band structure of non-strained $Ge_{1-x}Sn_x$ alloys with various Sn concentrations. The calculations show that at the Sn concentration of ~ 3.1 mol% the GeSn alloy presents a direct band gap. The variation of the band structure are ascribed to the weaker electro-negativity of Sn atoms and a slight charge transfer from Sn atoms to Ge atoms.

Keywords: GeSn alloy, direct band gap, first-principles calculation

PACS: 74.20.Pq, 71.20.Mq, 71.20.Nr **DOI:** 10.1088/1674-1056/26/12/127402

1. Introduction

Silicon (Si) and germanium (Ge) are most widely used semiconductors in the industry of integrated circuit. In recent years, the demands for photonics application and optoelectronic integration based on the two semiconductors have been increasing. However, the applications have been hindered by their indirect band gap. As shown in Fig. 1(a), the conduction band (CB) minimum of Si or Ge locates at the X or L point, respectively, while the valence band (VB) maximum locates at the center of the Brillouin zone, the Γ point. Among the two materials, Ge has a smaller separation between the direct gap and indirect gap, the direct CB valley at the Γ point is only ~ 140 meV above the indirect CB valley.[1,2] This small separation could be further reduced by means of heavy n-type doping,[3] tensile strain,[1,4–7] or alloys, and even an indirect–direct band gap transition could occur. Recent research efforts to achieve this aim focused on $Ge_{1-x}Sn_x$ (GeSn) alloys.[2,8–11] Sn-doping could effectively reduce the separation between the direct and indirect CB valleys, and the separation gradually reduces with increasing the fraction of Sn.[12–18] According to this tendency, at some critical concentration of Sn the direct and indirect CB valleys will reverse, i.e., GeSn alloy becomes a direct band gap semiconductor. However, the main challenge for the fabrication of GeSn alloys is the upper limit equilibrium solubility (< 1 mol%) of Sn in Ge,[9,19] which may result in Sn segregation in GeSn alloys with a high concentration of Sn. This problem was overcome by means of the epitaxial growth, and thick GeSn alloy films with a high concentration of Sn (> 10 mol%) were fabricated on diversified substrates.[13–18,20–23] Moreover, the mid-infrared LED and laser based on GeSn alloys were produced.[2,24] In most experiments the films of GeSn alloy were grown on Ge or Si substrate, suffering an in-plane compressive strain. This compressive strain increases the separation between the direct and indirect CB valleys, partially compensating the effect of Sn doping.[18] This implies that a higher Sn concentration is needed to realize a direct-gap band structure in GeSn alloys. Up to now, the direct band gap of GeSn alloy has been reported in several experiments, in which the lowest critical concentration of Sn for the indirect-to-direct band gap transition is about 8 mol%.[13,16]

Meanwhile, the band structure of GeSn alloys have also attracted much attention from theoretical research.[25–30] A first-principles calculation combined with the band-gap model of alloy predicted a critical Sn concentration of 6.3 mol%.[25] Most other calculations, which employed the empirical pseudopotential method combined with the virtual-crystal approximation (VCA), predicted the critical Sn concentrations varying from 6.5 mol% to 10 mol%. Noticeably, in the VCA the potential of Sn atoms is averagely distributed in the potential of Ge atoms, implying that the effect of the non-periodic potential arising from Sn atoms on the band structure is omitted. Up to now, the first-principles calculation based on real GeSn alloy atomic configurations has not been reported.

In this paper, to achieve a lower critical Sn concentration for the indirect–direct band gap transition, we study the band structure of non-strained GeSn alloys using hybrid-functional first-principles calculation. Instead of VCA method, we ap-

*Project supported by the Scientific Research Foundation for the Returned Overseas Chinese Scholars of the State Education Ministry of China (Grant No. [2015]-1098), the Open Project of the State Key Laboratory of Surface Physics of Fudan University, the Natural Science Foundation of Guangdong Province of China (Grant No. 2016A030307038), and the University Innovating and Strengthening Project of Department of Education of Guangdong Province, China (Grant No. 2015KTSCX090).

†Corresponding author. E-mail: liyunphy@foxmail.com

© 2017 Chinese Physical Society and IOP Publishing Ltd

ply the supercell method and band unfolding technique to perform the calculations of band structure, in which the effect of the non-periodic potential arising from Sn atoms on the band structure is properly considered. The results present a lower critical Sn concentration than the values reported so far.

2. Computational method

Our first-principles calculations were carried out using the Vienna *ab initio* Simulation Package (VASP) based on projector augmented wave approach within the framework of density functional theory.[31–33] The cut-off energy of plane wave basis set was 410 eV. Atomic structure optimizations were performed with the local-density-approximation (LDA) exchange–correlation functional.[34,35] To correctly evaluate the band gap, the electronic structure calculations were performed with the HSE06 hybrid functional[36–38] including 20% of the exact exchange energy and 80% of LDA exchange energy. The HSE06 hybrid functional has been applied extensively in first-principles calculation to correct the band gap of various semiconductor materials.[39–42] The valence electrons include Ge $3d^{10}4s^24p^2$ and Sn $4d^{10}5s^25p^2$. The Brillouin zone of Ge primitive cell was sampled by a Γ-centered $8\times8\times8$ $\boldsymbol{k}$-point mesh. The validity of the above calculation approach is confirmed by the good agreement between the calculated and experimental band structures of Ge. In the calculated band structure, as shown in Fig. 1(a), the indirect band gap E_g (L point) is 0.7 eV, the direct band gap E_Γ (Γ point) is 0.84 eV, and their difference $E_\Gamma - E_g$ is 0.14 eV. These values are in good agreement with the experimental values at 0 K, $E_g = 0.74$ eV, $E_\Gamma = 0.89$ eV, and $E_\Gamma - E_g = 0.14$ eV.[43] GeSn alloys with three Sn concentrations, 1/64, 1/32, and 1/16, were simulated with the supercells consisting of 64, 64, and 16 atoms, in which 1, 2, and 1 Sn atoms replace Ge atoms respectively. Γ-centered $3\times3\times3$, $3\times3\times3$, and $4\times4\times4$ $\boldsymbol{k}$-point meshs were used to sample the Brillouin zones. Both the stresses on the supercells and forces on all atoms were fully relaxed until the errors of total binding energy were less than 0.1 meV and the forces were less than 0.01 eV/Å. The supercell method leads to the band folding from the primitive-cell Brillouin zone into the smaller supercell Brillouin zone, bringing in an inconvenience when comparing the calculated band structure with the experimental one. Using the band unfolding technique the band levels of the supercell could be unfolded into the primitive-cell Brillouin zone, recovering an effective primitive-cell band structure.[44–48] In this paper, the band unfolding processes were performed using the Band-Up code.[48]

3. Results and discussion

Figure 1(a) displays the calculated band structure of Ge bulk, which presents an indirect band gap. Figures 1(b) and 1(c) display calculated effective band structures of two GeSn alloys with Sn concentrations of 1/64 and 1/16, respectively. Unlike the line-shape energy levels in Fig. 1(a), the energy levels in Figs. 1(b) and 1(c) present some broadening due to the non-periodic potential of Sn atoms, especially around the Γ point. The size of the filled circles represents the weight that an electron occupies the corresponding energy. Comparing with Ge bulk, the lowest CB level of GeSn alloys change remarkably. At the concentration of 1/64 [Fig. 1(b)] the direct CB valley at the Γ point lowers, nearly as high as the indirect CB valley at the L point. As Sn concentration increases to 1/16 [Fig. 1(b)], the direct CB valley at the Γ point is lower than the indirect CB valley at the L point, i.e., the GeSn alloy becomes a direct band-gap semiconductor. Our calculation shows that at Sn concentration of 1/32 the GeSn alloy also presents a direct-gap band structure with an E_g of 0.58 eV.

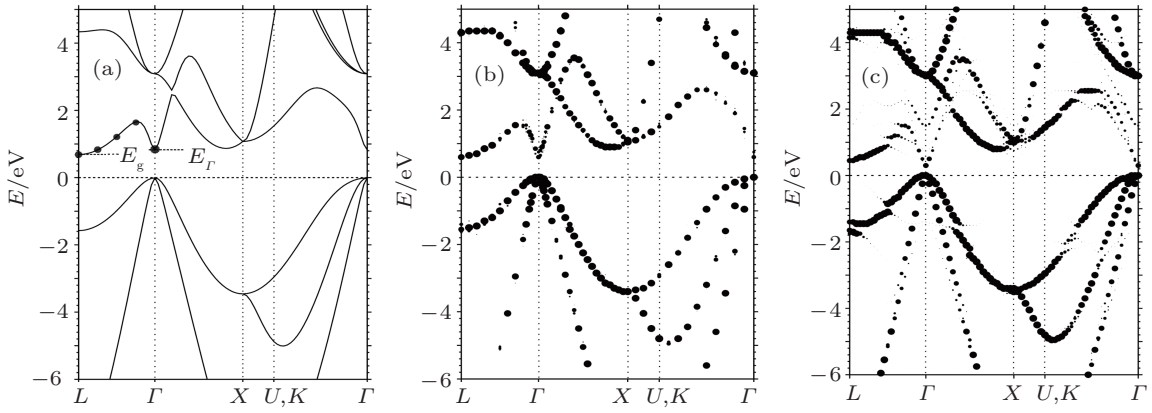


Fig. 1. (a) Calculated band structure of Ge bulk. (b) and (c) Calculated effective band structures of GeSn alloys with Sn concentrations of 1/64 and 1/16, respectively. The size of the filled circles in panels (b) and (c) represents the spectra weight that an electron occupies the corresponding energy.

Table 1 lists the values of the direct band gap of the three GeSn alloys. As Sn concentration increases from 1/64 to 1/32 and 1/16, the direct band gap reduces accordingly from 0.6 eV to 0.58 eV and 0.3 eV. The band structures in Figs. 1(b) and 1(c) show that with Sn concentration increasing the direct CB valley at the Γ point lowers more rapidly than the indirect CB

valley at the L point. Noticeably, our calculated critical concentration is about 1/32, i.e., $\sim$3.1 mol%, which is about a half of the value 6.3 mol%–6.5 mol% reported in previous calculations with VCA.[25,28] In addition, in GeSn alloys the lowest CB level at the Γ point broadens apparently. In Fig. 1(b) the spectra weight of the lowest CB level at the Γ is 0.5 and the broadening is 0.05 eV, and in Fig. 1(c) the spectra weight is 0.7 and the broadening is 1.2 eV. The spectra weight and broadening imply a lower intensity and larger broadening of light emission between the CBM and VBM. Table 1 also lists the lattice constants of the three GeSn alloys. With Sn concentration increasing the lattice constant increases gradually and the direct band gap decreases. This tendency is consistent with the results of compressive strained GeSn alloy films.[16]

Table 1. Calculated band gap E_g, and lattice constant ratio a/a_0 for GeSn alloys with various Sn concentrations n_d. Parameter a is the lattice constant of GeSn alloy and a_0 is the lattice constant of the pure Ge.

n_d	1/64	1/32	1/16
E_g/eV	0.60	0.58	0.30
a/a_0	1.0091	1.0094	1.0149

Figures 2(a) and 2(b) display the charge density of the CB valley at the Γ point for Sn concentration of 1/64 in Fig. 1(b). The charge distributes in the whole bulk rather than localizes near the Sn atom, implying a good electric conductivity. This property is also reflected by the large band dispersion of the CB valley at the Γ point shown in Figs. 1(b) and 1(c). The effective masses along [100] direction are 0.16 m_e and 0.28 m_e for Sn concentrations of 1/64 and 1/16, respectively. These values are close to the effective mass at the Γ point in Ge bulk, 0.09 m_e, and far less than the effective mass at the L point in Ge bulk, 1.59 m_e.

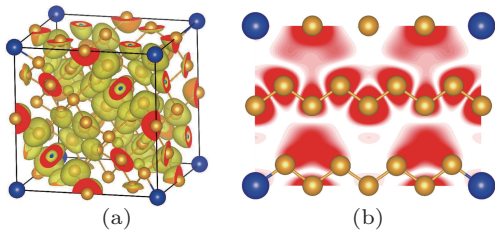


Fig. 2. (color online) Charge distribution of the conduction band valley at the Γ point in Fig. 1(b). (a) Isosurfaces, (b) contour on the (110) face. Coffee balls are Ge atoms, blue balls are Sn atoms.

To clarify how Sn doping changes the CB structure, we analyze the orbital constitution of the lowest CB level. Figure 3 displays partial densities of states (DOSs) of Ge and the GeSn alloy with Sn concentration of 1/64. The states near the CBM consist of Ge s and p orbitals. In Ge bulk the states of CBM consist of both Ge s and p orbitals, while in the GeSn alloy the states of CBM mainly consist of Ge s orbital. Figure 1(a) displays the orbital constitution of the lowest CB level along Γ–L $\boldsymbol{k}$-path, in which the size of filled circles represents the weight of Ge s orbital and the rest weight is contributed by Ge p orbitals. At the Γ point the weight of the s orbital is 1, i.e., the state of the CB valley at the Γ point only consists of Ge s orbital, while near the L point a part of Ge p orbitals mix into the level, i.e., s–p hybridization. In the tight-binding model the energy of the lowest CB level can be expressed approximately by

$$E = \varepsilon_s - J_s(\cos ak_x + \cos ak_y + \cos ak_z) - J_p(\cos ak_x + \cos ak_y + \cos ak_z),$$

in which J_s and J_p are overlap integrals of the periodic potential for nearest neighboring Ge s and Ge p orbitals, respectively. J_s is positive and J_p is negative because the s orbital has an even parity and the p orbitals have an odd parity. Along the $\boldsymbol{k}$-path from the Γ to L (π/a, π/a, π/a) the overlap integral of the s orbitals rises up the level, while that of the p orbitals lowers the level much more so that the energy at the L point is lower than that at the Γ point. In contrast, in the GeSn alloy [Fig. 1(c)] the situation inverses, i.e., the energy of the level at the Γ point is lower than that of the L point. This implies that the Sn-doping weakens the overlap integral of Ge p orbitals relatively.

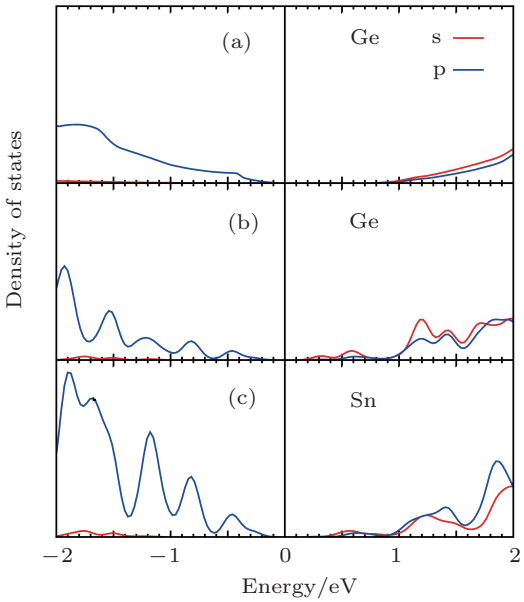


Fig. 3. (color online) Partial densities of states of (a) Ge atom in Ge bulk, (b) the Ge atom at the center of Ge63Sn1 supercell shown in Fig. 2(a), and (c) Sn atom of Ge63Sn1.

Figure 4 displays that the difference of electrostatic potential energy between GeSn alloy with Sn concentration of 1/64 and Ge bulk. The potential near Ge atom in the GeSn alloy is slightly higher than that of the Ge atom in Ge bulk. This is caused by a slight charge transfer from Sn atom to Ge atom in GeSn alloy because the electro-negativity of Sn atom is weaker than Ge atom. The extra charge occupying Ge p orbitals weakens the valence bond between Ge atoms and lower

the weight of p orbitals in the lowest CB level as well. This reduces the overlap integral of Ge p orbitals, i.e., J_p, therefore relatively raising the energy of the CB valley at the L point. Moreover, the positive-charged Sn atom and neighboring negative-charged Ge atoms slightly break the periodicity of the lattice potential and therefore lead to scattering of the electron in the CB valley at the Γ point. The former lowers the energy of a part of states of the CB valley at the Γ point, while the latter lifts the energy of some states, therefore leading to a broadening of the level at the Γ point as shown in Figs. 1(b) and 1(c). In addition, the Sn-doping also increases the lattice constant. The expansion of lattice weaken the bond of Ge s orbital as well as p orbitals, lowering overall the conduction band, i.e., the band gap reduces with Sn concentration increasing.

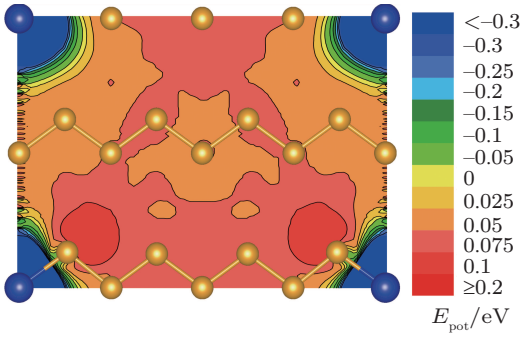


Fig. 4. (color online) Difference of electrostatic potential energy E_{pot} between Ge63Sn1 and Ge64 on (110) face. Coffee balls are Ge atom and blue balls are Sn atom.

4. Summary

We have investigated the band structure of non-strained GeSn alloys with various Sn concentrations using the hybrid-functional first-principles calculation combined with the supercell method and band unfolding technique. The calculation results show that at the Sn concentration of ~ 3.1 mol% the GeSn alloy becomes a direct-gap semiconductor and the energy level of the conduction band minimum at the Γ point presents a large broadening. The change of the conduction band originate from the weaker electro-negativity of Sn atom and induced charge transfer from Sn atom to Ge atom, which weakens the bonds between Ge p orbitals more than Ge s orbitals and therefore change the dispersion of the lowest conduction band level.

Acknowledgement

Yun Li thanks the support by the Scientific Research Foundation for the Returned Overseas Chinese Scholars of State Education Ministry (Grant No. [2015]-1098). Yun Li and Xinyuan Wei thank the support by the Open Project of State Key Laboratory of Surface Physics of Fudan University. Chengzhao Chen thanks the supports by the Natural Science Foundation of Guangdong Province of China (Grand No. 2016A030307038) and the University Innovating and Strengthening Project of Department of Education of Guangdong Province, China (Grand No. 2015KTSCX090). Yun Li thanks W Ku for helpful discussions.

References

[1] Shen H, Li D S and Yang D R 2015 *Acta Phys. Sin.* **64** 204208 (in Chinese)
[2] Wirths S, Geiger R, von den Driesch N, Mussler G, Stoica T, Mantl S, Ikonic Z, Luysberg M, Chiussi S, Hartmann J M, Sigg H, Faist J, Buca D and Grützmacher D 2015 *Nat. Photon.* **9** 88
[3] Liu L, Sun X, Pan D, Wang X, Kimerling L C, Koch T L and Michel J 2007 *Opt. Express* **15** 11272
[4] Süess M J, Geiger R, Minamisawa R A, Schiefler G, Frigerio J, Chrastina D, Isella G, Spolenak R, Faist J and Sigg H 2013 *Nat. Photon.* **7** 466
[5] Sun X, Liu J, Kimerling L C and Michel J 2009 *Appl. Phys. Lett.* **95** 011911
[6] Sanchez-Perez J R, Boztug C, Chen F, Sudradjat F F, Paskiewicz D M, Jacobson R, Lagally M G and Paiella R 2011 *Proc. Natl. Acad. Sci.* **108** 18893
[7] Nam D, Sukhdeo D, Roy A, Balram D, Cheng S L, Huang K C Y, Yuan Z, Brongersma M, Nishi Y, Miller D and Saraswat K 2011 *Opt. Express* **19** 25866
[8] Homewood K P and Lourenco M A 2015 *Nat. Photon.* **9** 78
[9] He G and Atwater H A 1997 *Phys. Rev. Lett.* **79** 1937
[10] D'Costa V R, Cook C S, Birdwell A G, Littler C L, Canonico M, Zollner S, Kouvetakis J and Menéndez J 2006 *Phys. Rev. B* **73** 125207
[11] Mathews J, Beeler R T, Tolle J, Xu C, Roucka R, Kouvetakis J and Menéndez J 2010 *Appl. Phys. Lett.* **97** 221912
[12] Tseng H H, Wu K Y, Li H, Mashanov V, Cheng H H, Sun G and Soref R A 2013 *Appl. Phys. Lett.* **102** 182106
[13] Chen R, Lin H, Huo Y, Hitzman C, Kamins T I and Harris J S 2011 *Appl. Phys. Lett.* **99** 181125
[14] Wirths S, Ikonic Z, Tiedemann A T, Holländer B, Stoica T, Mussler G, Breuer U, Hartmann J M, Benedetti A, Chiussi S, Grützmacher D, Mantl S and Buca D 2013 *Appl. Phys. Lett.* **103** 192110
[15] Gencarelli F, Vincent B, Demeulemeester J, Vantomme A, Moussa A, Franquet A, Kumar A, Bender H, Meersschaut J, Vandervorst W, Loo R, Caymax M, Temst K and Heyns M 2013 *ECS J. Solid State Sci. Technol.* **2** 134
[16] Senaratne C L, Gallagher J D, Aoki T and Kouvetakis J 2014 *Chem. Mater.* **26** 6033
[17] Oehme M, Kostecki K, Schmid M, Oliveira F, Kasper E and Schulze J 2014 *Thin Solid Films* **557** 169
[18] von den Driesch N, Stange D, Wirths S, Mussler G, Hollaänder B, Ikonic Z, Hartmann J M, Stoica T, Mantl S, Grützmacher D and Buca D 2015 *Chem. Mater.* **27** 4693
[19] Thurmond C D, Trumbore F A and Kowalchik M J 1956 *Chem. Phys.* **25** 799
[20] Gupta S, Chen R, Huang Y C, Kim Y, Sanchez E, Harris J S and Saraswat K C 2013 *Nano Lett.* **13** 3783
[21] Tao P, Huang L, Cheng H H, Wang H H, and Wu X S 2014 *Chin. Phys. B* **23** 088112
[22] Mahmodi H and Hashim M R 2017 *Chin. Phys. B* **26** 056801
[23] Vincent B, Gencarelli F, Bender H, Merckling C, Douhard B, Petersen D H, Hansen O, Henrichsen H H, Meersschaut J, Vandervorst W, Heyns M, Loo R and Caymax M 2011 *Appl. Phys. Lett.* **99** 152103
[24] Kasper E and Oehme M 2015 *Jpn. J. Appl. Phys.* **54** 04DG11
[25] Yin W J, Gong X G and Wei S H 2008 *Phys. Rev. B* **78** 161203
[26] Low K L, Yang Y, Han G, Fan W and Yeo Y C 2012 *J. Appl. Phys.* **112** 103715
[27] Kotlyar R, Avci U E, Cea S, Rios R, Linton T D, Kuhn K J and Young I A 2013 *Appl. Phys. Lett.* **102** 113106
[28] Gupta S, Magyari-Köpe B, Nishi Y and Saraswat K C 2013 *J. Appl. Phys.* **113** 073707
[29] Lan H S and Liu C W 2014 *Appl. Phys. Lett.* **104** 192101
[30] Sant S and Schenk A 2014 *Appl. Phys. Lett.* **105** 162101
[31] Kresse G and Furthmuller J 1996 *Comput. Mater. Sci.* **6** 15

[32] Blöchl P E 1994 *Phys. Rev. B* **50** 17953
[33] Kresse G and Joubert D 1999 *Phys. Rev. B* **59** 1758
[34] Ceperley D M and Alder B J 1980 *Phys. Rev. Lett.* **45** 566
[35] Perdew J P and Zunger A 1981 *Phys. Rev. B* **23** 5048
[36] Heyd J, Scuseria G E and Ernzerhof M 2003 *J. Chem. Phys.* **118** 8207
[37] Heyd J and Scuseria G E 2004 *J. Chem. Phys.* **121** 1187
[38] Heyd J, Scuseria G E and Ernzerhof M 2006 *J. Chem. Phys.* **124** 219906
[39] Liu B, Wu L J, Zhao Y Q, Wang L Z, and Cai M Q 2016 *J. Magn. Magn. Mater.* **420** 218
[40] Wu L J, Zhao Y Q, Chen C W, Wang L Z, Liu B and Cai M Q 2016 *Chin. Phys. B* **25** 107202
[41] Wang L Z, Zhao Y Q, Liu B, Wu L J and Cai M Q 2016 *Phys. Chem. Chem. Phys.* **18** 22188
[42] Liu B, Wu L J, Zhao Y Q, Wang L Z and Cai M Q 2016 *RSC Adv.* **6** 92473
[43] http://www.ioffe.ru/SVA/NSM/Semicond/Ge/bandstr.html
[44] Wang L W, Bellaiche L, Wei S H and Zunger A 1998 *Phys. Rev. Lett.* **80** 4725
[45] Popescu V and Zunger A 2012 *Phys. Rev. B* **85** 085201
[46] Ku W, Berlijn T and Lee C C 2010 *Phys. Rev. Lett.* **104** 216401
[47] Zheng G, Zhang P and Duan W 2015 *Comput. Phys. Commun.* **189** 213
[48] Medeiros P V C, Stafström S and Björk J 2014 *Phys. Rev. B* **89** 041407